

## CHAPTER 3

### EXPERIMENTAL CHARACTERISATION OF FLUID-INDUCED VIBRATION CHARACTERISTICS

As described in Chapter 2, the two most dangerous types of flow-induced vibration are fluid-elastic instability and flow periodicity. After consultation with the manufacturer, it became evident that fluid-elastic instability was already being addressed in cases where it could provide problems, i.e. heat exchangers with large flexible panels in high flow-velocities.

The flow periodicity however, had not been addressed by the manufacturer, as the cases in which large deflections would result under operational conditions, have more specific requirements. These requirements include that periodicity frequency must closely correspond to the natural frequency of the heat exchanger plates.

In the literature study it was found that there existed a number of studies on either vortex shedding of plates and panels, or the flow structure over dimples in channels (Ligrani, Harrison, Mahmood, & Hill, 2001; Ligrani, Mahmood, Harrison, Clayton, & Nelson, 2001; Mahmood & Ligrani, 2002), but there is no study that examined the combined effects of panel with dimples and the frequency spectrum of the excited vibration.

An experiment was therefore devised to provide some insight into the forcing frequency spectrum that is a result of the two combined mechanisms. Rather than building an exact model of the heat exchanger, which would be costly, and very complex, taking into account among others the surface finish, material thickness and dimple geometry, it was decided to opt for a more qualitative study and determine general features of the forcing frequency spectrum for a dimpled panel in axial flow.

The qualitative features that were expected to be outcomes of the experiment included whether both the expected mechanisms would provide measurable excitation, which mechanism would be responsible

for the largest forces and what the order of magnitude of the frequencies would be.

### 3.1. Design of the experiment

The structure of the dimple plates was simulated by heating 1,5 mm Perspex sheets to 160°C and then forming the sheets over a mould using EPDM sponge to simulate the same constant pressure process as the air-pressure used in the manufacture of the metal dimple plates. Figure 11 illustrates the formed Perspex plate mounted on the model.

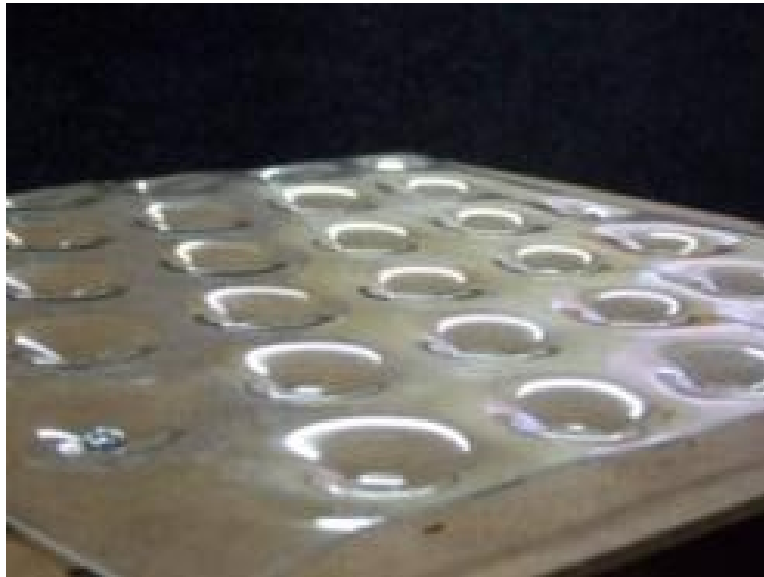


**Figure 11: Formed Perspex sheet to simulate dimples in heat exchanger**

Because this process created only one side of the dimple plate, two sheets were glued together to form a complete dimpled panel.

To simulate the flow pattern between the plates, the complete dimpled panel was fixed in a cantilever configuration between two shaped sheets, as shown in Figure 12.



**Figure 12: Flow model assembly, dimple plate between two formed Perspex sheets**

The dimpled panel was, therefore, subject to the same flow that was experienced in the plate pack of a dimple plate heat exchanger, while it was free to vibrate between the outer plates. The forcing frequency could then be determined with an acceleration meter mounted on the central plate.

By adjusting the distance between the plates ( $H$ ), the aspect ratio of the dimpled channel could be altered.

Figure 13 illustrates the resulting dimples with a diameter ( $D$ ) of approximately 30 mm at a triangular pitch of 80 mm. This resulted in the finished dimpled panel having a thickness of approximately 20 mm.

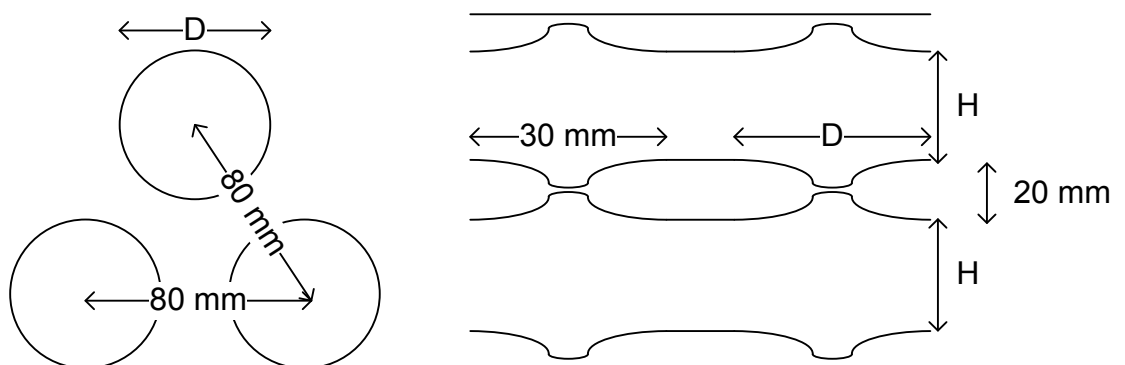


**Figure 13: Geometry of resulting dimples**

The height of the channel ( $H$ ) could be adjusted to control the aspect ratio of the plate pack ( $H/D$ ), which was the non-dimensional measure of the channel height used in the experiments.

### 3.2. Characterisation of parameters

The model was mounted in the flow passage of a sub-sonic wind tunnel as illustrated in Figure 14. The tunnel was adjustable for airflow speeds of between 6 and 24 m/s, which provided adequate test values as the operational flow velocities for the dimple plate heat exchangers were between 5 and 50 m/s.



Figure 14 : The flow-model mounted in the wind tunnel

#### 3.2.1. Wind velocity

The velocity of the wind was set by a dial on the blower in increments between a setting of 1 and 12. The adjustment dial of the blower can be seen in Figure 15.



Figure 15: The blower dial that adjusts the wind velocity

Without taking the blockage factor of the model into account, the velocity of the wind at the test section was varied between  $6 \text{ m}\cdot\text{s}^{-1}$  and  $25.1 \text{ m}\cdot\text{s}^{-1}$ .

Table 1 indicates the resulting wind speed for the corresponding blower settings.

**Table 1: Comparison between blower settings and wind velocities**

Setting	Wind Velocity [m/s]
1	6
2	6.8
3	7.8
4	8.4
5	9.4
6	10.8
7	12.2
8	14
9	16.1
10	18.7
11	21.6
12	25.1

### 3.2.2. Background vibration

As the wind tunnel was not designed specifically for fluid-induced vibration measurements, the blower and speed control gearbox caused vibration at the test bed, which was not caused by the fluid structure interaction. The vibration of the wind tunnel test bed had to be determined in order to evaluate which vibrations were transferred to the model via the test bed and which were flow-induced.

The vibration caused by the blower and gearbox was measured on the blower case where the tunnel was connected to the wind tunnel. The setup during the experimental measurement can be seen in Figure 16.

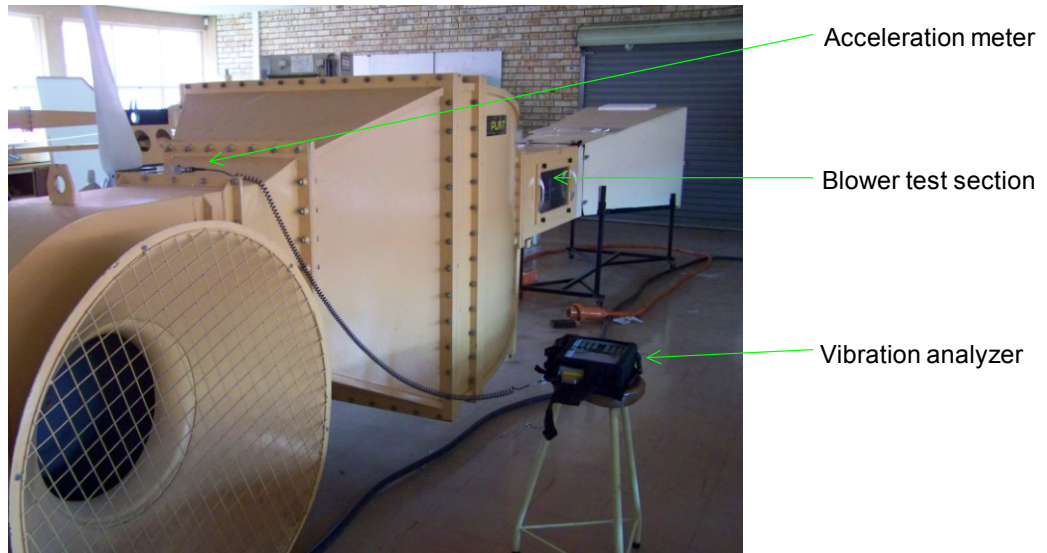


**Figure 16: Measurement of background vibration on the blower channel**

Figure 17 illustrates the measured vibration spectra for all the blower settings together in a waterfall graph.

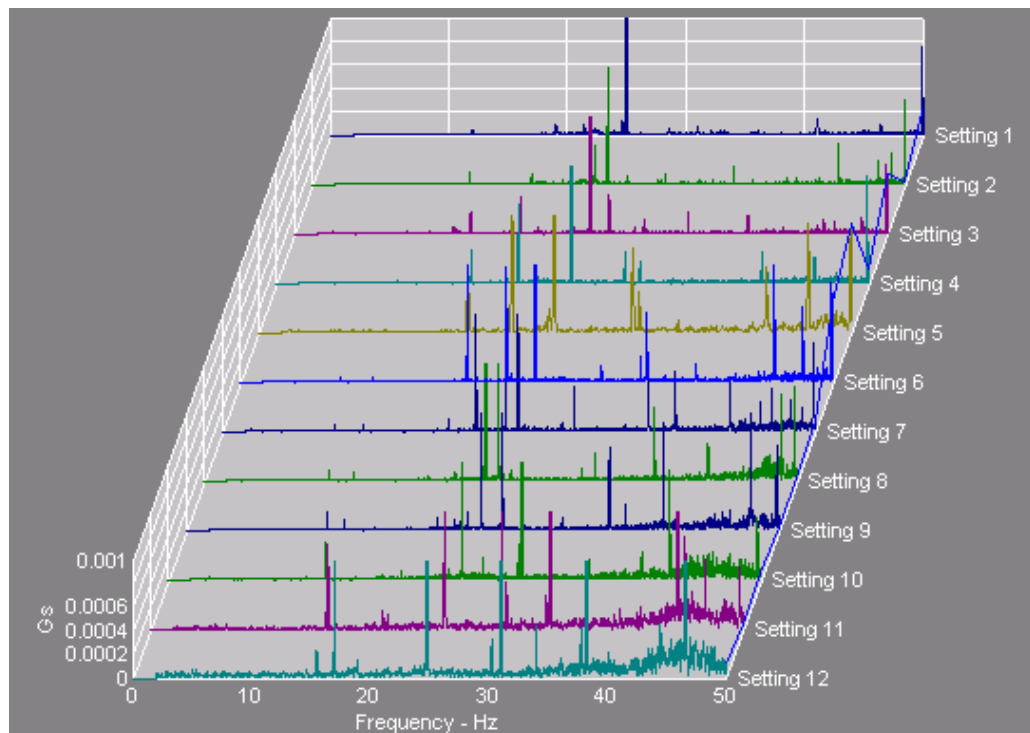


**Figure 17: Measured background vibration measured on the blower channel**

From the range of spectra the running speed of the motor could be seen at all settings as a constant peak at 25 Hz (standard running speed of 4 pole motor). A further number of varying peaks could be seen that were possibly caused by gear mesh frequencies of the gear box and vane

pass frequencies of the blower. All these peaks either had a positive linear or higher-order relationship with the wind tunnel setting and the wind speed.

### 3.2.3. Natural frequencies

To interpret the results of the experiment correctly, the natural frequency of the dimpled panel in the model had to be measured experimentally.

After adjusting the height of the channel to an aspect ratio ( $H/D$ ) of 2, as defined in Figure 13, the dimpled panel was excited under static conditions with a rubber mallet. The natural response was measured by using a Microlog vibration analyser and a 100 mV SKF accelerometer. The time and frequency spectrum results are illustrated in Figure 18 and Figure 19.

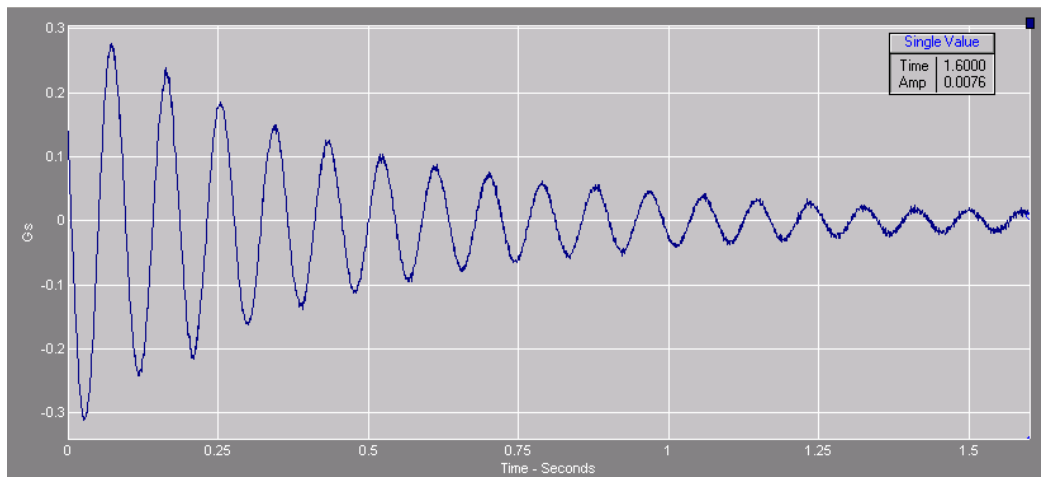


**Figure 18: Time spectrum response of the bump test performed for aspect ratio of 1**

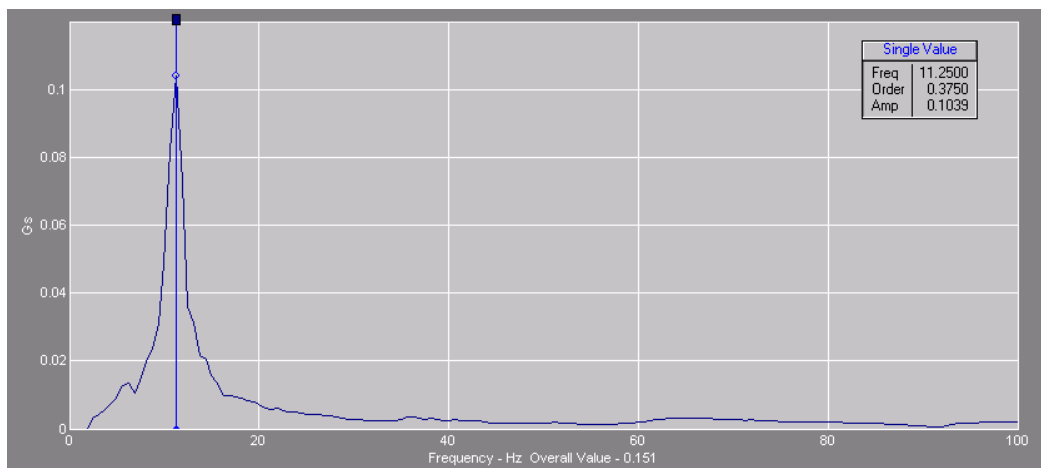


**Figure 19: Frequency spectrum response of the bump test for aspect ratio of 2**

From these results, it was evident that the natural frequency of the plate assembly, with an aspect ratio ( $H/D$ ) of 2, was established to be 11.25 Hz.

The same procedure was used to determine the natural frequency after the aspect ratio ( $H/D$ ) of the experiment had been reduced to 1. The results can be seen in Figure 20 and Figure 21.

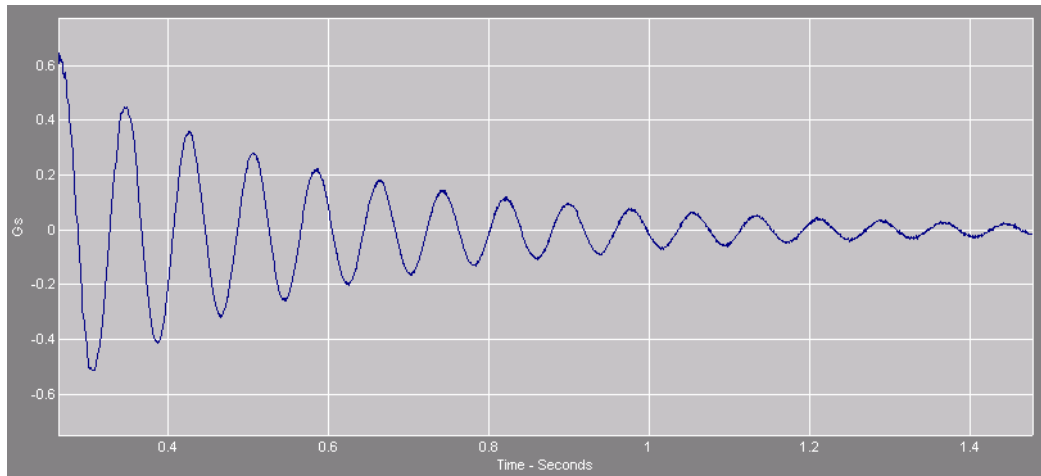


**Figure 20: Time spectrum response for the bump test performed for aspect ratio of 1**

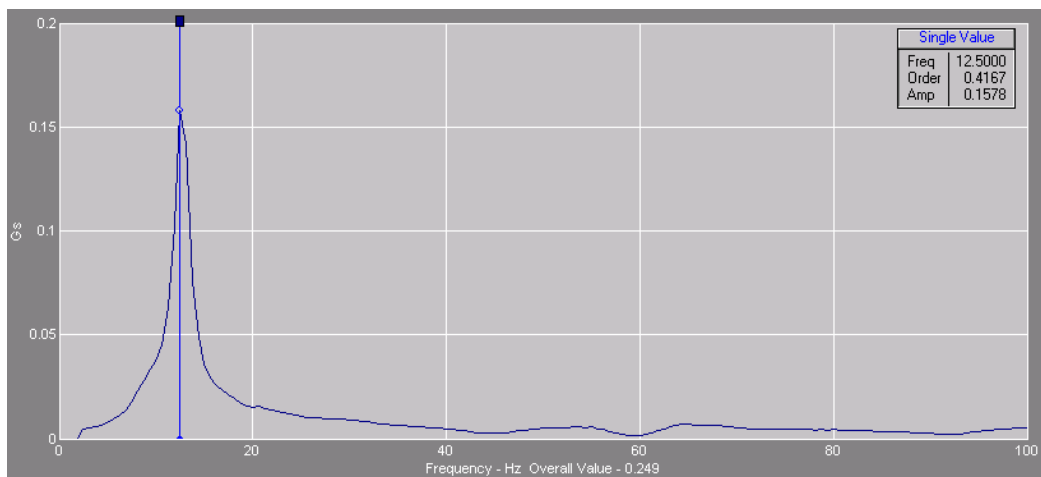


**Figure 21: Frequency spectrum response for the bump test performed for aspect ratio of 1**

Due to the decrease in the length of the struts and the resulting increase in stiffness, the natural frequency for aspect ratio of 1 increased from 11.25 Hz measured in the previous case, to a value of 12.5 Hz.

### 3.3. Experimental evaluation

Once the background vibration and the natural frequency of the plates had been determined, the experimental work could commence. The response of the central panel was captured and analysed in the frequency domain by a vibration analyser for the entire range of flow velocities. This process was repeated for both the aspect ratios, so that the results could be compared.

#### 3.3.1. $H/D = 2$

With the approximate dimple diameter of 30 mm, the panels were adjusted for a channel height (H) of 60 mm. With the distance between the plates set to the required aspect ratio of 2, the model was mounted in the blower channel as can be seen in Figure 22.



Figure 22: Model for aspect ratio of 2 with mounted accelerometer

The measured vibration on the middle panel for the range of blower settings and an aspect ratio of 2 is graphically illustrated in Figure 23.

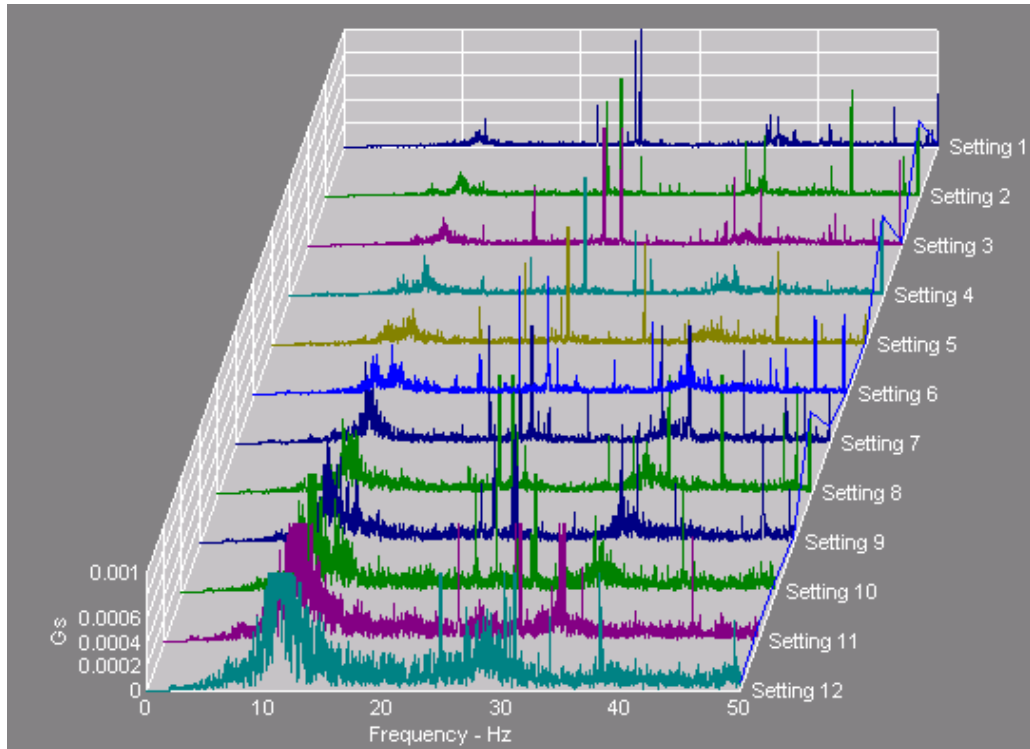


**Figure 23: Vibration measurements of dimpled panel with aspect ratio of 2**

It is immediately evident that two bands of peaks are present in these spectra that were not evident in the range of background spectra of Figure 17. The first prominent band was easily identified as the natural frequency of the dimpled panel, measured during characterisation as 11.25 Hz.

Another prominent band of peaks is evident between 30 and 40 Hz. To prove that the bands of peaks were indeed induced by the fluid flow over the dimpled panel, the background vibration spectrum was studied between 30 and 40 Hz. Figure 24 is an enlargement of the measured vibration response over the relevant range of frequencies and clearly shows the range of peaks.

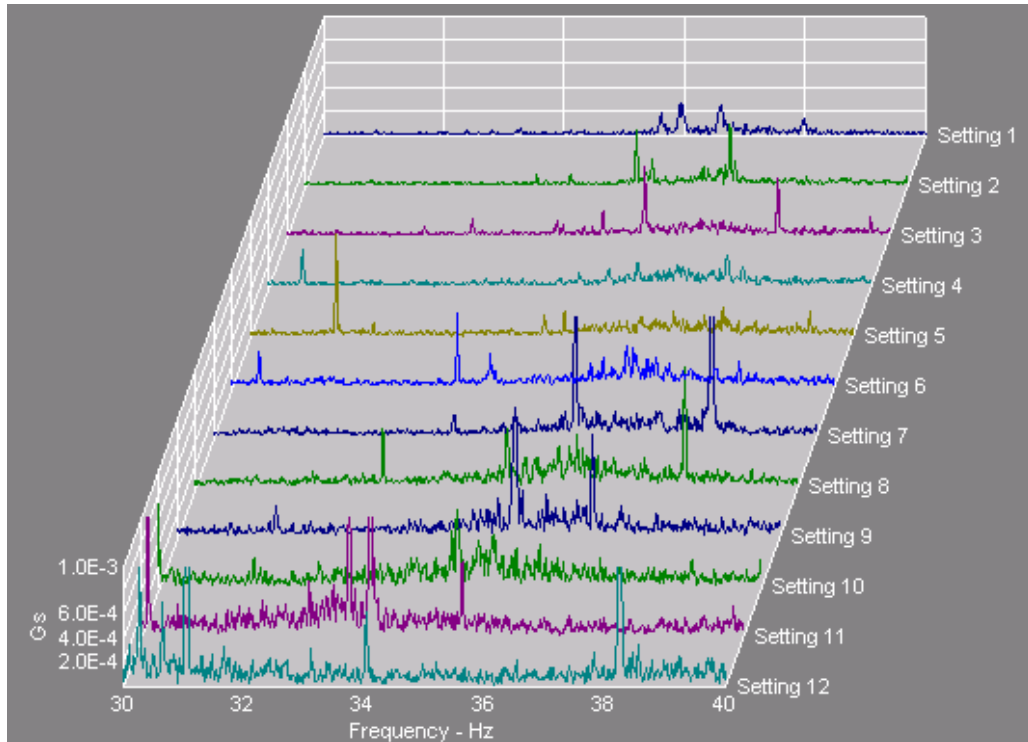


**Figure 24: Measured vibration of dimpled panel for aspect ratio of 2, between 30 and 40 Hz**

Figure 25 is an enlargement of the vibration measurements taken on the blower channel as illustrated fully in Figure 17. It is clearly indicated that there is no range of peaks evident in the background vibration between 30 Hz and 40 Hz that compared to the band of peaks identified in Figure 24.

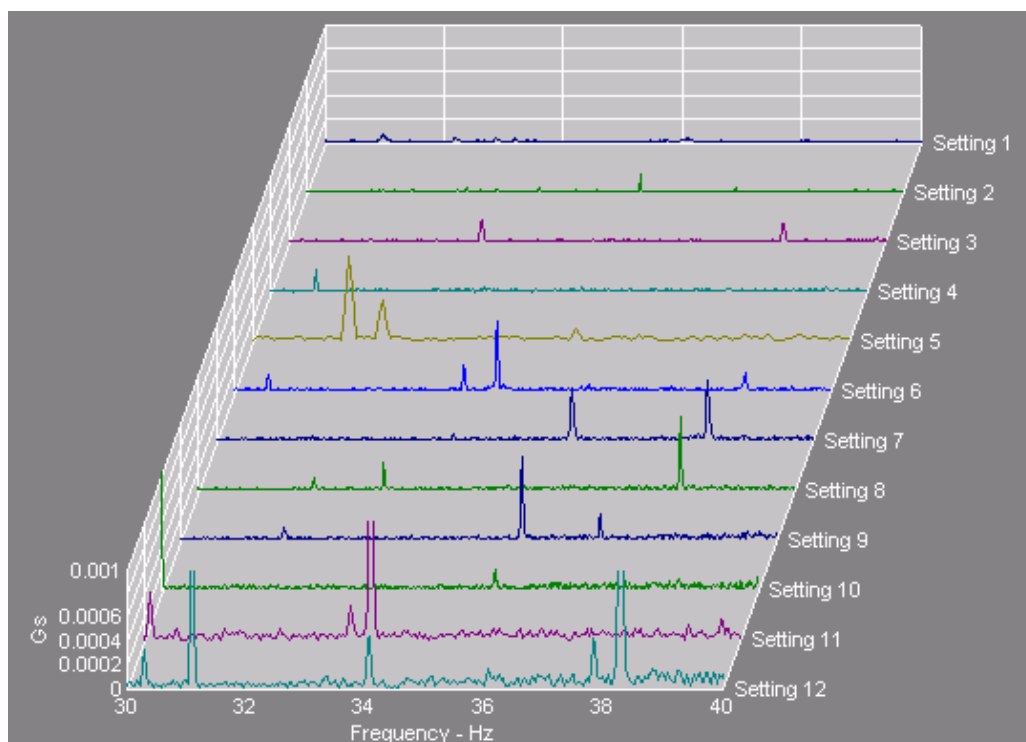


**Figure 25: Measured vibration spectra of blower channel between 30 and 40 Hz**

The band of peaks illustrated in Figure 24 differed with regard to the characteristic of the background vibration amplitude, as the indicated range of peaks reduced in frequency as the wind velocity increased. The normal background bands of peaks increased exponentially with the increase of wind velocity. This fact further indicated that the source of the two different bands of peaks was indeed different. This promoted the idea that this range of frequencies was flow-induced.

On the measured vibration spectra of the dimpled panel, a third, less conspicuous, band of peaks can be seen ranging from just below the natural frequency of the dimpled plates from about 8.7 Hz to approximately 15 Hz. This range of peaks can only be seen if the measured vibration spectra of the dimpled panel (as illustrated in Figure 23) were enlarged around 10 Hz, as illustrated by Figure 26.

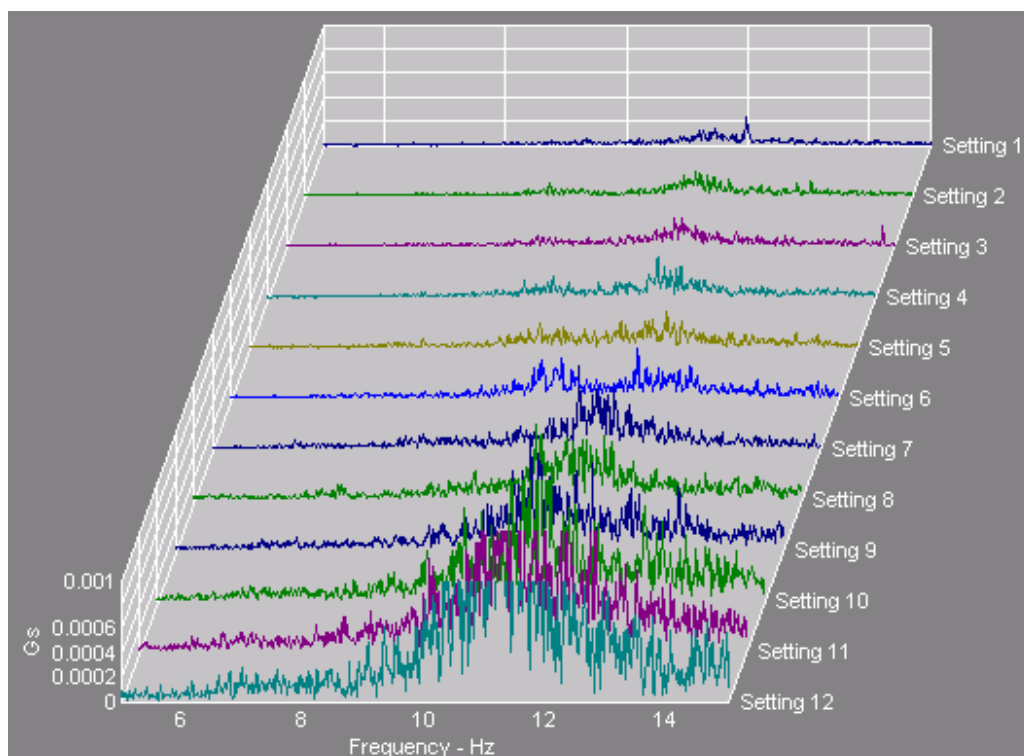


**Figure 26: Measured vibration spectra of the panels between 5 and 15 Hz**

In the figure the natural frequency of the panels can be identified as a constant peak at 11.25 Hz and that the unidentified band of peaks starts at values below the natural frequency and increases past the natural frequency. It can further be seen that resonance occurs when the band of peaks coincide with the natural frequency of the panels. This resonance results in a visible increase of the amplitude of vibration in the measurements from setting 7 and higher.

### 3.3.2. $H/D = 1$

With the approximate dimple diameter of 30mm, the panels were adjusted to a channel height of 30 mm to create an aspect ratio of 1. After the panels had been adjusted to the new aspect ratio, the model was mounted in the blower channel in exactly the same way as in the previous case. The experimental setup can be seen in Figure 27.



**Figure 27: Experimental setup for an aspect ratio of 1**

From the experimental setup the range of the vibration spectra for the forced vibration of the dimpled plate with an aspect ratio of 1 was determined. These vibration measurements are illustrated simultaneously on a waterfall graph in Figure 28.

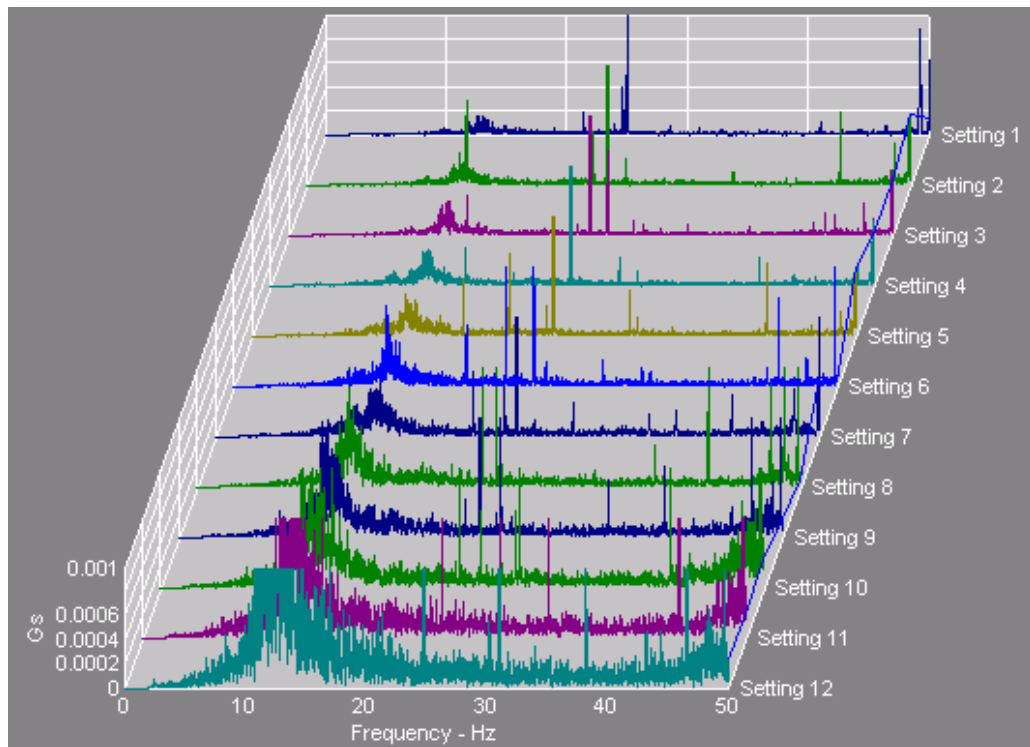


**Figure 28: Vibration response of the dimpled plate with aspect ratio of 1**

From the characterisation of the model with an aspect ratio of 1, the natural frequency of the plates was identified at 12.5 Hz.

The range of peaks evident between 30 and 40 Hz in the previous case was absent; on further inspection a range was identified at a higher frequency, between 45 Hz and 65 Hz. By zooming in on the waterfall graph on this specific range of frequencies, the range of peaks became evident, as illustrated in Figure 29.

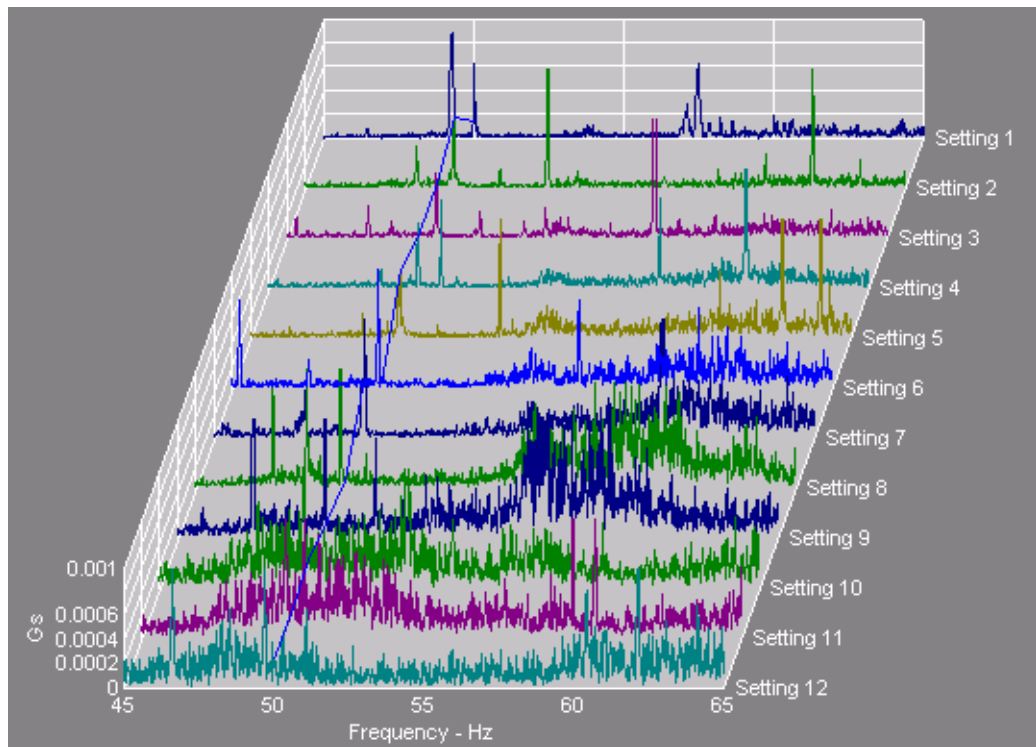


**Figure 29: Measured response between 45 and 65 Hz for aspect ratio of 1**

This band of peaks shows a reverse exponential relationship with the wind tunnel setting, with the frequency value of the peaks reducing with the increase of the wind tunnel settings and, therefore, the wind velocity over the dimpled panel. This characteristic was also evident in the band of peaks illustrated in Figure 24 for the other aspect ratio.

To ensure that the band of peaks in question was induced by the flow over the dimpled panel, the same range of frequencies was enlarged for the background vibration measurements. Figure 30 illustrates that bands of peaks cannot be identified in the same location in the vibration measurements on the blower channel. It can, therefore, be concluded that the vibrations causing the band of peaks were flow-induced.

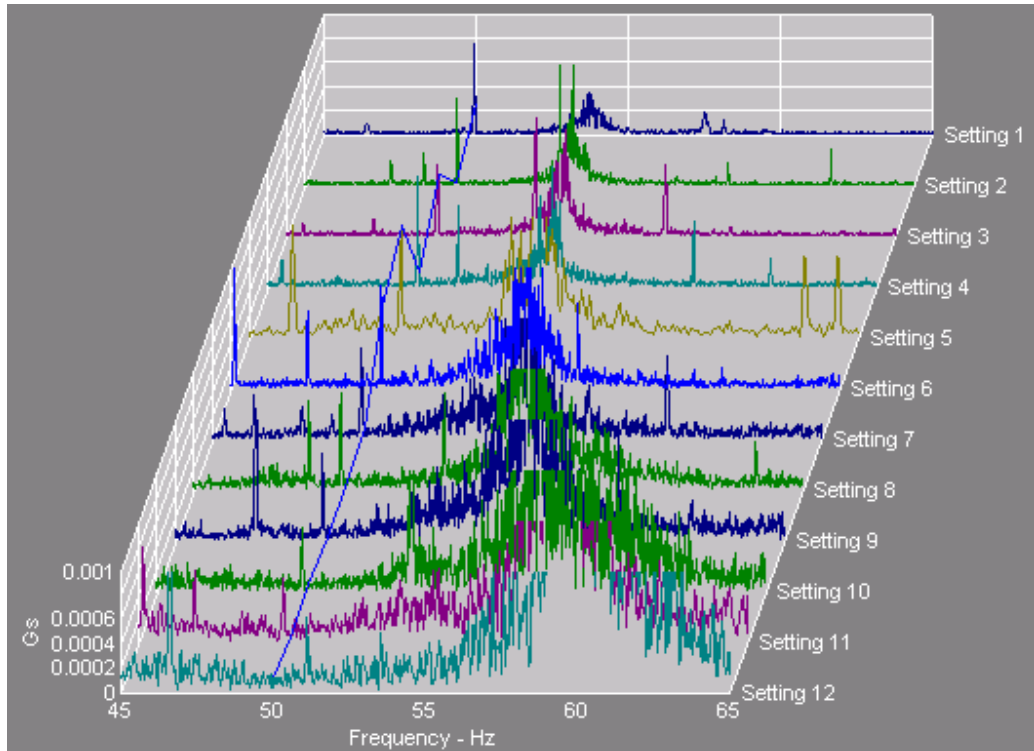


**Figure 30: Measured vibration of the blower channel between 45 and 65 Hz**

As in the case where the panels were set up with an aspect ratio of 2, illustrated by Figure 26, a band of peaks were evident just below the natural frequency of the panel when the aspect ratio was set to 1. The range of frequencies around the natural frequency of the panels is illustrated in Figure 31.

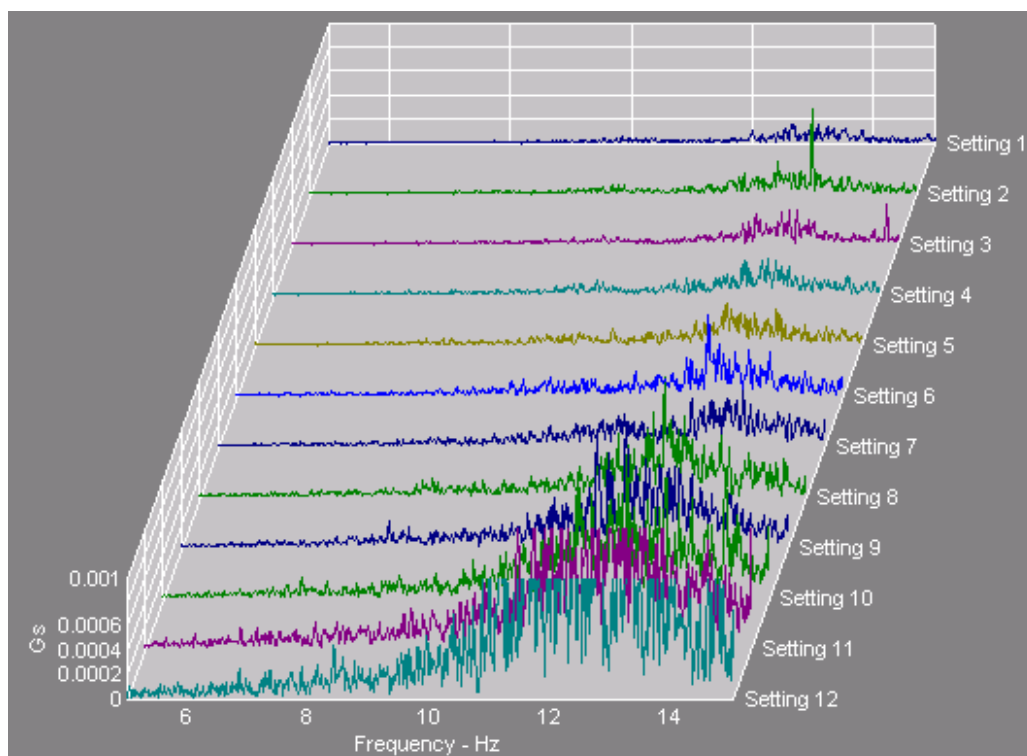


**Figure 31: Measured response between 5 and 15 Hz**

The band of peaks appears to start a little higher (9.9 Hz) than in the previous case, illustrated by Figure 26.

The amplitude of the peaks was small until the peaks came close to the natural frequency of the plates. As in the previous case, once the peaks cross the natural frequency (at approximately Setting 8), the intensity of the vibration increased visibly. This indicates the occurrence of resonance when the band of peaks is close to the natural frequency of the panels.

### 3.4. Conclusion

From the results of the experiments two ranges of peaks were evident in the spectra that was measured, which were not present in the background vibration that was measured on the blower channel. It can, therefore, be concluded that these two ranges of peaks are fluid-induced vibrations in the dimpled panel.

As flow periodicity was the most likely cause of these vibration ranges, the attributes of the vibration ranges was studied to determine which type of flow periodicity was responsible for the range of peaks.

The lowest range of peaks increased with the wind velocity and increased slightly with a decrease in aspect ratio. This band of peaks was only moderately affected by the aspect ratio of the model, but increased with the increased velocity. This conforms to what is expected from the vortex shedding frequency of the plates.

The second, more prominent range of peaks, was evident in the case where the aspect ratio was 2 (30 – 40 Hz). In the case where the aspect ratio was 1, a band of peaks with the same characteristics could be identified at a higher frequency (45 – 65 Hz).

The fact that the frequency band was higher at the smaller aspect ratio, leads to the conclusion that the source of vibration was affected by the aspect ratio. As the frequency decreased when the wind velocity increased, the band was consistent with vortex ejection, where the frequency decreased with an increase in Reynolds number.

This experiment, though not quantitative, revealed certain important qualities of vibration caused by flow periodicity.

- Two forms of flow-induced vibration could be identified in the same dimpled panel that was distinguishable from the background turbulence.
- The vibration with the higher frequency value caused the largest vibration amplitude, but when the lower frequency was close to the natural frequency of the panel, there was a marked increase in the amplitude of peaks present.
- As these excitation frequencies were confined to definite bands of higher vibration, the amplitude of the vibration could easily be reduced by isolating the system in such a way that the response to forcing vibrations in those regions remained small.

The experimental studies conducted by Ligrani, *et al.* (2001) found that the frequency of the vortex ejection was substantially lower than that measured in this experiment. This difference could have been caused by the interaction between the movement of the plates due to vortex shedding, or the dimples at the top of the channel.

The small size of the vortex shedding peaks (lower range of peaks) can most probably be attributed to the high turbulence of the flow emanating from the dimpled channel. This, however, did not decrease the effect of the vibration if it coincided with the natural frequency of the plate pack.

It is evident from this simple experiment that there is an opportunity to study the types of vibrations caused by dimple plates in axial flow in more detail. Transient computational fluid dynamics and more accurate non-dimensional models of industrial heat exchangers mounted on a test bed isolated from the vibration caused by the blower could be used.